Olive mill solid waste induces beneficial mushroom-specialized metabolite diversity: a computational metabolomics study

Soliman Khatib[1,2*], Idan Pereman[2,3*], Elizabeth Kostanda[3], Mitja M. Zdouc[4], Nirit Ezov[3], Ron Schweitzer[1,2], and Justin J. J. van der Hooft[4,5*]

[1]Natural Compounds and Analytical Chemistry Laboratory, MIGAL – Galilee Research Institute, Kiryat Shemona, Israel

[2]Department of Biotechnology, Tel-Hai College, Upper Galilee 12210, Israel

[3]Molecular biology and analytics of medicinal mushrooms Laboratory, MIGAL – Galilee Research Institute, Kiryat Shemona, Israel

[4]Bioinformatics Group, Wageningen University & Research, Droevendaalsesteeg 1, 6708 PB Wageningen, the Netherlands

[5]Department of Biochemistry, University of Johannesburg, Johannesburg, 2006, South Africa

* Corresponding authors: Soliman Khatib (solimankh@migal.org.il), Idan Pereman (idanpe@migal.org.il), Justin J. J. van der Hooft (justin.vanderhooft@wur.nl)

Abstract

Hericium erinaceus and *Pleurotus eryngii* are edible and medicinal mushrooms grown commercially in many countries around the world. In nature, *H. erinaceus* grows on old or dead trunks of hardwood trees. *P. eryngii* grows on the roots of Apiaceae plants. To exploit their beneficial properties, these mushrooms have been grown indoors using mushroom substrates mainly consisting of dry wood chips, straw, and cereals originating from forest maintenance, agriculture, and industry wastes, respectively. Additional supplements such as olive mill solid waste are added to the substrate to support mushroom development. However, the impact of substrate additives on the edible mushroom metabolic content has not been assessed so far. We examined the effect of adding to the substrate different proportions of olive mill solid waste on the metabolic profiles of the fruiting body (FB) and mycelium of *H. erinaceus* and *P. eryngii* mushrooms. We used computational metabolomics methods to analyze the untargeted metabolomics data obtained from Q-Exactive Plus high-resolution LC-MS/MS data. In general, the methanolic extracts of *H. erinaceus* FB and mycelium were more highly enriched with specialized metabolites than those of *P. eryngii*. Interestingly, olive mill solid waste increased some of the unique metabolites related to the beneficial hericenone family in the *H. erinaceus* FB and several erinacerin metabolites from the mycelium. At the same time, the additive decreased the toxic enniatin metabolite abundance. Altogether, we demonstrate how a change in substrate composition affects the mushroom's specialized metabolome and can induce beneficial mushroom metabolite diversity. This highlights the importance of including metabolomics strategies to investigate new sustainable growth options for edible mushrooms and other natural foods.

Introduction

Mushrooms are familiar food ingredients, not only due to their unique flavor and texture, but also due to their beneficial effects on human health[1,2]. For thousands of years, mushrooms have been used to support health, especially in East Asian countries[3]. In recent years, major biological constituents in edible/medicinal mushrooms have been explored for their health-related beneficial properties, including macromolecules (e.g., polysaccharides, polysaccharide–proteins/peptides and proteins) and low-molecular-weight molecules (e.g., cerebrosides, isoflavones, catechols, amines, triacylglycerols, sesquiterpenes and steroids)[4,5].

Hericium erinaceus, an edible and medicinal mushroom, is widely consumed in Asian countries[6]. Its fruiting body (FB) and mycelium are used in traditional Chinese medicine for the treatment of gastritis and hyperglycemia[7]. The pharmacological benefits of *H. erinaceus*, including antiaging, antioxidant, antitumor, antidiabetic, antidementia, antidepression[8] and antianxiety activities[9-12], are due to its large number of bioactive secondary metabolites, such as phenols (hericenones), aromatic compounds (hericerins, erinacerins and erinaceolactones), sterols, polysaccharides and glycoproteins[13,14]. *Pleurotus eryngii* is an edible mushroom which is cultivated for commercial use in many countries around the world. It has rapidly become a highly valued species in North Africa, Europe and Asia, in part due to its meaty structure that makes it a popular meat substitute. Many extracts from *P. eryngii* have been studied *in vivo* and *in vitro*, demonstrating interesting biological activities of the mushroom, including anticancer, antioxidant, antimicrobial, hypoglycemic and immunostimulatory effects[15-17]. In nature, *H. erinaceus* grows on old or dead trunks of hardwood trees. *P. eryngii* grows on the roots of Apiaceae plants. Typically, in an industrial setting, mushrooms grow indoors on substrates that mainly include dry plant materials (sawdust, dry wood chips, cereals etc.) which commonly originate in agricultural and industrial wastes. Usually, a nitrogen source such as soybean hulls or grains can be added to the substrate to promote optimal mushroom development. In an effort to find a solution for polluting by products originating in the oil industry, Olive Mill Solid Waste (OMSW) was tested as an efficient nitrogen-contributing component[18,19]. As a matter of fact, the olive oil industry produces extensive amounts of highly polluting by-products, both water waste and solid waste. Olive oil extraction can generate up to 30–40% OMSW and much effort has been invested in its exploitation[20,21].Here, it is important to note that the type or characteristics of the growing substrate significantly influence the content of certain bioactive compounds in the mushrooms[22,23]. For example, recent studies have exhibited an increase in

the healthy and beneficial glucans alpha and beta concentrations in correlation with the addition of several concentrations of olive mill waste to the substrate[24].

Hence, in the present study, we grew *H. erinaceus* and *P. eryngii* on a mushroom substrate mixed with OMSW to explore the effect of OMSW addition on the mushroom's metabolite profile and the possible impact on the consumers that may have.

High-resolution (HR) LC-MS/MS untargeted metabolomics is an important method for analyzing small-molecule metabolites present in a biological sample in a particular physiological state, currently one of the most rapidly evolving research fields. Untargeted metabolomics can provide a "snapshot" of the sample, by identifying and quantifying small molecules metabolites. Many studies have made use of untargeted metabolomics to analyze plant samples, and some have investigated mushrooms[25,26]. To facilitate the analysis and interpretation of the complex datasets obtained from HRLC-MS/MS in untargeted metabolomics, computational metabolomics methods are employed. The area of computational metabolomics focuses on applying computational, statistical, and machine-learning methods to analyze and interpret metabolomic data and its integration with other datasets, such as various omics or clinical data[27,28]. In the present study, we assessed the effect of OMSW on metabolite-profile diversity in the FB and mycelium of *H. erinaceus* and *P. eryngii* mushrooms using computational metabolomics methods to analyze the HRLC-MS/MS data. The results can be used to assess if the use of various growth resources for mushrooms are desirable by studying the impact on their edible constituents.

Methods

Mushroom growth conditions

P. eryngii and *H. erinaceus* were grown on a sterilized mixture of eucalyptus sawdust (originating from forest management cut-wood piles in northern Israel) and OMSW (collected from a local olive-oil production factory), with the addition of malt waste (collected from a local beer production factory). OMSW, the solid fraction from a three-phase olive mill, was added at concentrations of 0% (w/w) to 80% (w/w). The mixture was wetted to 52–58% water content and packed into 2 L polypropylene bags containing a microporous filter, 0.8 kg wet substrate/bag. The bags were autoclaved at 121°C for 1 h and cooled to 25°C for inoculation with grain spawn. The culture was incubated at 23.5°C for 14–21 days.

For fruiting, the bags were opened, and the temperature was reduced to 18°C, with a relative humidity of 90% and 8 h of light daily.

FB were freshly harvested at the Matityahu Experimental Farm (Upper Galilee, Israel). They were collected according to their maturity level (spines elongation in *H. erinaceus*, cap opening in *P. eryngii*). After harvest, FB and spent mushroom substrate (SMS) were weighed, chopped into small pieces, and freeze-dried.

Table 1. The four experimental groups of growth media with varying concentrations of OMSW.

	80%	**60%**	**33%**	**0%**
OMSW (%)	80	60	33	0
Malt (%)	10	20	33	50
Eucalyptus (%)	10	20	33	50
Water content (%)	52	54	56	58

Extraction conditions

All samples of FB, SMS, and mushroom substrate were ground using a mechanical grinder, briefly vortexed and extracted in methanol (MeOH; analytical, suitable for LC-MS) at a ratio of 1:20 (1 g of dried material in 20 ml MeOH). The extraction was performed by shaking at 25°C and 1000 rpm for 2 h. After extraction, the samples were centrifuged (4°C, 3220*g* for 30 min) and the liquid was collected and filtered through a 0.45-µm syringe filter; 1 mL of the filtered extract was kept in a LC-MS vial at -80°C while the remaining extract was dried in an evaporator (for yield calculation). Dry extracts were kept at -20°C.

HPLC analysis

The samples were analyzed by injecting 5 µl of the extracted solutions into a Dionex Ultimate 3000 ultra-HPLC system connected to a photodiode array detector (Thermo Fisher Scientific), with a reverse-phase column (ZORBAX Eclipse Plus C18, 100 x 3.0 mm, 1.8 µm; Agilent). The mobile phase consisted of (A) 0.1% formic acid in DDW and (B) 0.1% formic acid in MeOH. The gradient began at 95% A which was kept isocratic for 1 min, then decreased to 40% B over 2 min and kept isocratic for 2 min, then increased to 97% B over 8 min and kept isocratic at 97% B for another 19.5 min. Phase A was returned

to 95% over 1.5 min and the column was allowed to equilibrate at 95% A for 3 min before the next injection. The flow rate was 0.4 mL/min.

LC–MS/MS analysis

MS/MS analysis was performed with a heated electrospray ionization (HESI-II) source connected to a Q Exactive Plus Hybrid Quadrupole-Orbitrap mass spectrometer (Thermo Fisher Scientific). ESI capillary voltage was set to 3000 V, capillary temperature to 350ºC, gas temperature to 350ºC and gas flow to 35 mL/min. The mass spectra (m/z 100–1000) were acquired in negative- and positive-ion modes with high resolution (FWHM = 70,000). MS^1 parameters were: resolution 70,000, AGC target $3E^6$, maximum IT 100 ms, scan range 67–1000 m/z; MS^2 parameters were: resolution 17,500, AGC target $1E^5$, maximum IT 50 ms, loop count 5, MSX count 1, isolated window 1, collision energy (N)CE 20, 50 and 80 EV; data dependent (dd) settings were: minimum AGC $8E^3$, apex trigger 6 to 16 s, exclude isotope on, dynamic exclude 8.0 s.

Computational metabolomics analysis

Data reprocessing

Data-dependent MS/MS spectrum files were converted from .raw to .mzXML using the GNPS vendor-conversion (Mass Spectrometry File Conversion – GNPS Documentation; ccms-ucsd.github.io)[29]. Data preprocessing was performed using MZmine 3.3.0 software and included the following steps: mass1 and mass2 detection with noise levels of $4.0E^5$ and $1.0E^4$ respectively, LC-MS chromatogram building and resolution with intensity threshold of $9.0E^5$ and minimum highest intensity of $2.0E^6$, isotope grouping, alignment, isotope pattern filtering, gap filling and filtering out of duplicate peaks[30], M/Z and RT tolerance were set to 5 and 0.5 respectively. More details about MZmine 3 parameters can be found in the batch file in the supplementary data. The aligned feature lists were exported to the GNPS platform as MS/MS files (.mgf format) and quantification tables (.csv format of aligned features and related chromatographic peak areas).

FERMO analysis

FERMO_0.8.8 dashboard[31] (permanently available from https://zenodo.org/records/7565701) was used for the prioritization of molecular features from the MS data which were upregulated or downregulated upon addition of OMSW. The MS/MS file (.mgf format) and full quantification table (.csv format) were

obtained from MZmine 3 analysis using the 'Export molecular networking files (e.g., GNPS, FBMN, IIMN, MetGem)' export button. Feature intensity was set to 'Height'. The parameters used for the FERMO analysis were: mass deviation 5; minimum number of fragments per MS^2 spectrum 5; QuantData factor 2; Blank factor 10; relative intensity filter range 0.01–0.95; spectral similarity networking algorithm, modified-cosine; fragment similarity tolerance 0.1; fragment similarity tolerance 0.8. MS2Query was used to annotate the MS/MS data[32].

Molecular networking analyses

Molecular networks were obtained using the feature-based molecular networking (FBMN) workflow[33] in GNPS (https://gnps.ucsd.edu,). The precursor ion mass tolerance was set to 0.02 Da and the MS/MS fragment ion tolerance to 0.01 Da. A molecular network was then created where edges were filtered to have a cosine score above 0.6 and more than 4 matched peaks. The maximum size of a molecular family was set to 100. The spectra in the network were then searched against GNPS spectral libraries[29,34]. The library spectra were filtered in the same manner as the input data. All retained matches between network spectra and library spectra were required to have a score above 0.5 and at least 4 matched peaks. DEREPLICATOR+[35], Network Annotation Propagation (NAP)[36] and Structural Similarity Network Annotation Platform for Mass Spectrometry (SNAP-MS) were used to annotate MS/MS spectra[37]. The molecular networks were visualized using Cytoscape software[38].

MolNetEnhancer Workflow for chemical class annotation of molecular networks

To elaborate on the chemical structure information in a molecular network, information from in-silico structure annotations generated by GNPS library search, NAP and DEREPLICATOR+ was incorporated into the network using the GNPS MolNetEnhancer workflow[39] (https://ccms-ucsd.github.io/GNPSDocumentation/molnetenhancer/) on the GNPS website (http://gnps.ucsd.edu). Chemical class was annotated using ClassyFire chemical ontology[40].

Data deposition and job accessibility

The MS data were deposited in the public repository MassIVE: positive ionization mode in (MSV000090919), and negative ionization mode in (MSV000090920). The molecular networking jobs can be publicly accessed and browsed at the following URLs: https://gnps.ucsd.edu/ProteoSAFe/status.jsp?task=069e4c5dc7d846a4a96e485091d199a4 for *Hericium*,

https://gnps.ucsd.edu/ProteoSAFe/status.jsp?task=60727fe5228643e6a482bd797d83df38 for *Pleurotus* and https://gnps.ucsd.edu/ProteoSAFe/status.jsp?task=2b86dd35cc4a4219bad07c3519ad78bf for *Hericium* and *Pleurotus* together.

Results and discussion

H. erinaceus mushrooms were grown on sterilized substrate comprised of eucalyptus sawdust and malt waste mixed with different percentages of OMSW (0%, 33%, 60% and 80%). FB, SMS and mushroom substrates were collected, extracted, and analyzed by HRLC-MS/MS. Mushroom substrates with 0%, 33%, 60% and 80% OMSW were used as blanks to filter out non-biological signals. The effect of OMSW on mushrooms growth and development was reported previously [18,19]. In the present study the impact of the OMSW on mushrooms specialized metabolite diversity was examined using computational metabolomics approaches.

Use of MZmine 3 for LC-MS/MS data processing in positive ionization mode led to the detection of 2766 and 1899 features in the *H. erinaceus* and *P. eryngii* mushroom sample extracts, respectively, for which MS/MS data was collected and that were further analyzed by FBMN and subsequently prioritized using the FERMO dashboard.

FERMO platform to prioritize *Hericium* FB metabolites affected by OMSW

FERMO dashboard was used to prioritize metabolites that were upregulated or downregulated with increasing OMSW percentage in the mushroom substrate. Molecular features were also detected in the mushroom substrate blanks containing 0%, 33% 60% and 80% OMSW, yellow-colored peaks in Figure 1A were removed as they cannot be mushroom-generated, leaving 360 features in the *Hericium* FB extracts (Fig. 1B). From these, 56 features were selected with over 2-fold higher quantity (signal intensity) in the mushrooms grown with 80% OMSW compared to those grown with 0% (Fig. 1C and Fig. S1). Most of these selected features were connected in two molecular families based on mass spectral similarity networking, and their quantities increased dose-dependently with increasing percentage of the OMSW (Fig. S1). This increase was significant for 18 of the metabolite features (Fig. S2).

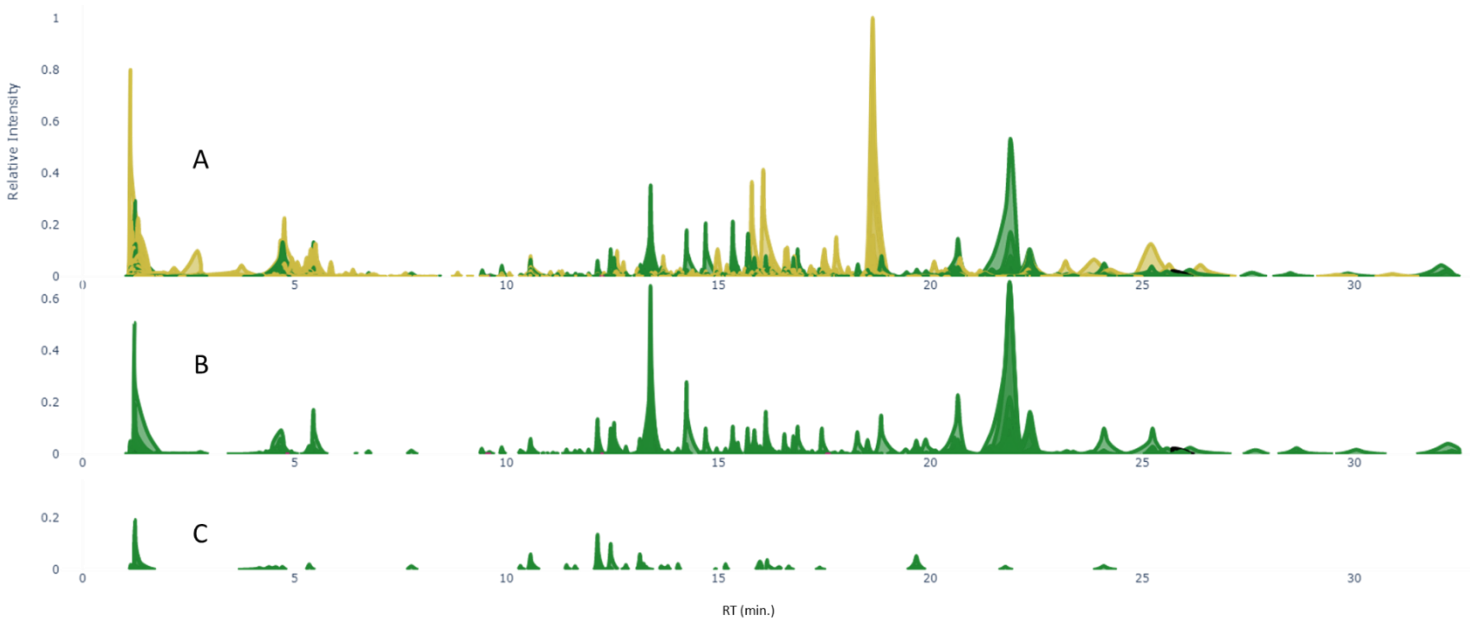

Fig. 1. FERMO analysis of MS data from extracts of *Hericium* mushrooms grown on substrate with different percentages of OMSW. (A) Pseudo chromatogram of molecular features detected in extracts of *Hericium* fruiting bodies (FB) grown on mushroom substrate mixed with 80% OMSW (green), and features detected in the mushroom substrates medium blank samples (yellow). (B) Pseudo chromatogram of molecular features detected in extracts of *Hericium* FB after blank removal. (C) Pseudo chromatogram of molecular features with 2-fold higher quantity in the FB extracts of *Hericium* grown on 80% OMSW compared to 0% OMSW.

Three of the metabolites that increased with the addition of OMSW were annotated using MS2Query, with a score higher than 0.7 and Δm/z = 0, as acetyl carnitine (A), (4aR,10aR)-6,7-dihydroxy-1,1,4a-trimethyl-3,4,10,10a-tetrahydro-2H-phenanthren-9-one (B) and 6-[(3E,5E,7S)-5,7-dimethyl-2-oxonona-3,5-dienyl]-2,4-dihydroxy-3-methylbenzaldehyde (C) (Fig. 2 A–C, G). Two metabolites were annotated by DEREPLICATOR+ as the *Hericium*-unique metabolites hericenones F (D) and hericenone G (E), with scores of 12 and 15, respectively (Fig. 2G); their quantities did not change by the addition of OMSW (Fig. 2 D and E). A metabolite whose quantity decreased significantly in a dose-dependent manner with the addition of OMSW was annotated by DEREPLICATOR+ to be pregn-5-ene-3,14,20-triol_3-O-[3-O-methyl-α-D-galactopyranosyl-(1→4)-β-D-digitoxopyranoside] (F) with a DEREPLICATOR+ score of 7 (Fig. 2G). Interestingly, none of these metabolites were annotated with a MS2Query score higher than 0.7, showing the complementarity of existing annotation strategies. In addition, 64 features were selected mainly in the 0% OMSW group, with only traces of these metabolites detected in the FB grown on mushroom substrates mixed with OMSW (Fig. S3).

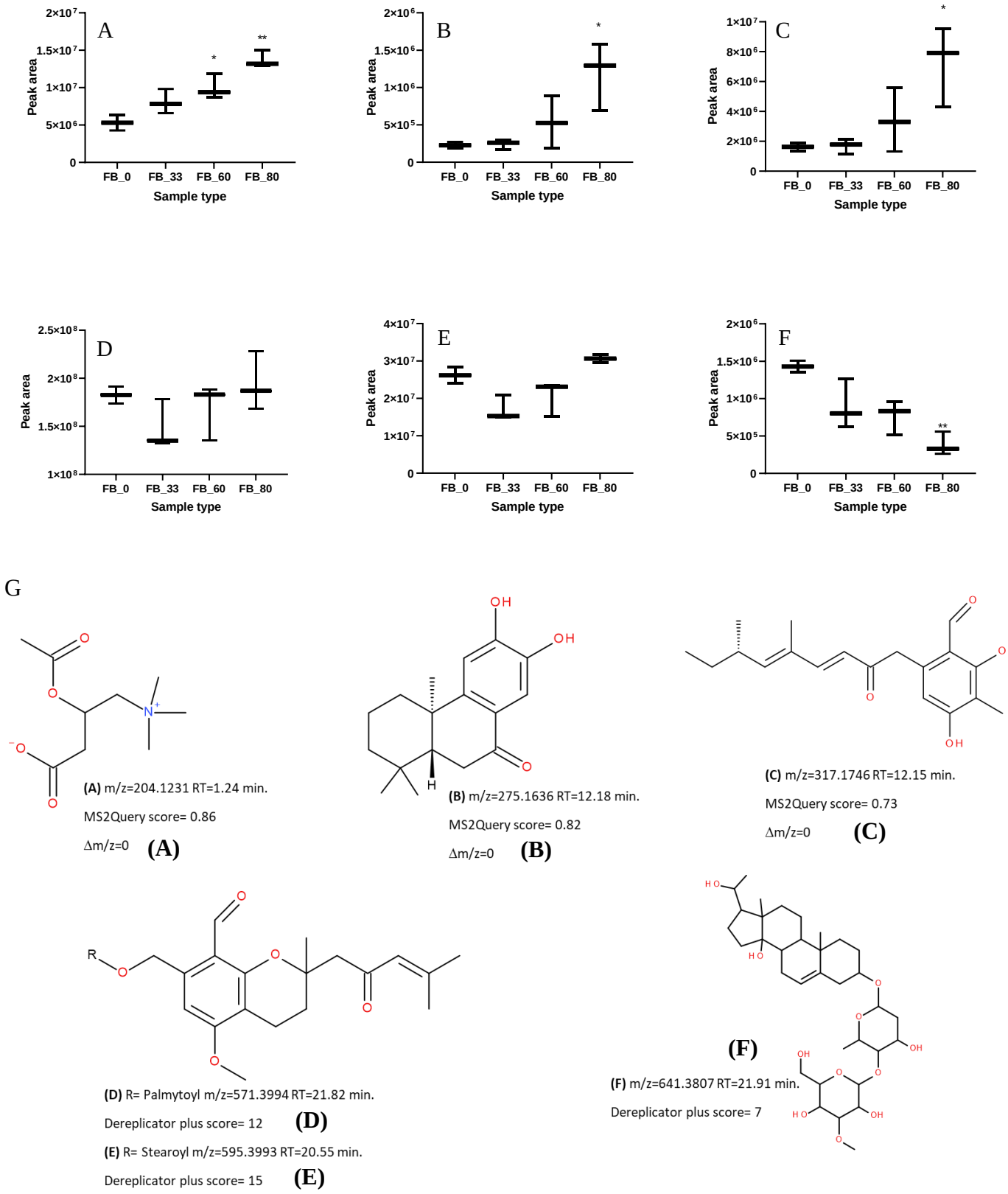

Fig. 2. (A, B and C) Box and whisker plots of selected metabolites whose quantities were significantly increased in the *Hericium* fruiting body (FB) with increasing percentage of OMSW in the mushroom substrate. (D and E) Metabolites whose quantities did not change in the FB with increasing OMSW in the mushroom substrate. (F) A

metabolite that significantly decreased in the FB with increasing OMSW percentage in the mushroom substrate. The figures present the mean area values ± SD from three extracts for each group (n = 3). *$P \leq 0.05$, **$P \leq 0.01$ relative to the 0% OMSW FB group. Statistical analysis was carried out by one-way ANOVA and GraphPad Prism 9 software. (G) Metabolite structures annotated using MS2Query or DEREPLICATOR+.

FBMN for the analysis of *Hericium* and *Pleurotus* mushrooms

FBMN was used to analyze the LC-MS/MS data of the extracts obtained from the *Hericium* and *Pleurotus* FB, SMS and mushroom substrates (without mycelium). First, the LC-MS/MS data of the extracts was processed using MZmine 3 to obtain 2766 and 1899 features for *Hericium and Pleurotus*, respectively followed by an analysis using FBMN on the GNPS platform. Of the obtained features, 1258 and 1837 were connected by molecular networks for *Pleurotus* and *Hericium*, respectively (Figs. S4 A and B). After removing molecular networks that included features from mushroom substrates mixed with 0%, 33%, 60% and 80% OMSW without mushroom mycelium (blank features), 752 and 240 features remained for the FB and mycelium of *Hericium* and *Pleurotus*, respectively (Fig. S4 C and D).

Of the 240 features obtained from the *Pleurotus* FBMN analysis, 153 were annotated using GNPS libraries, 33 of them with confidence higher than 95%; 153 were annotated using NAP and 142 were annotated using DEREPLICATOR+, 84 of the latter with a score higher than 10 (Fig. S5A). *Pleurotus* FB and mycelium exhibited a relatively limited number of secondary metabolites. Molecular family classification using ClassyFire showed that the majority belonged to phospholipids (22%), amino acid and carboxylic acid derivatives (15%), steroids (15%), sphingolipids (10%) and fatty acids (8%) (Fig. S5B).

Of the 752 features obtained from the *Hericium* FBMN analysis, 165 were annotated using GNPS libraries, 28 of them with confidence higher than 95%; 165 were annotated using NAP and 406 were annotated using DEREPLICATOR+, 221 of the latter with a score higher than 10 (Fig. 3A). FBMN analysis showed that *Hericium* FB and mycelium were richer in specialized secondary metabolites than *Pleurotus*. About 40% of the *Hericium* secondary metabolites belonged to the prenol lipids, which distributed into coumarins, sesterterpenoids, triterpenoids, diterpenoids and diterpene lactones (Fig. 3 B and C).

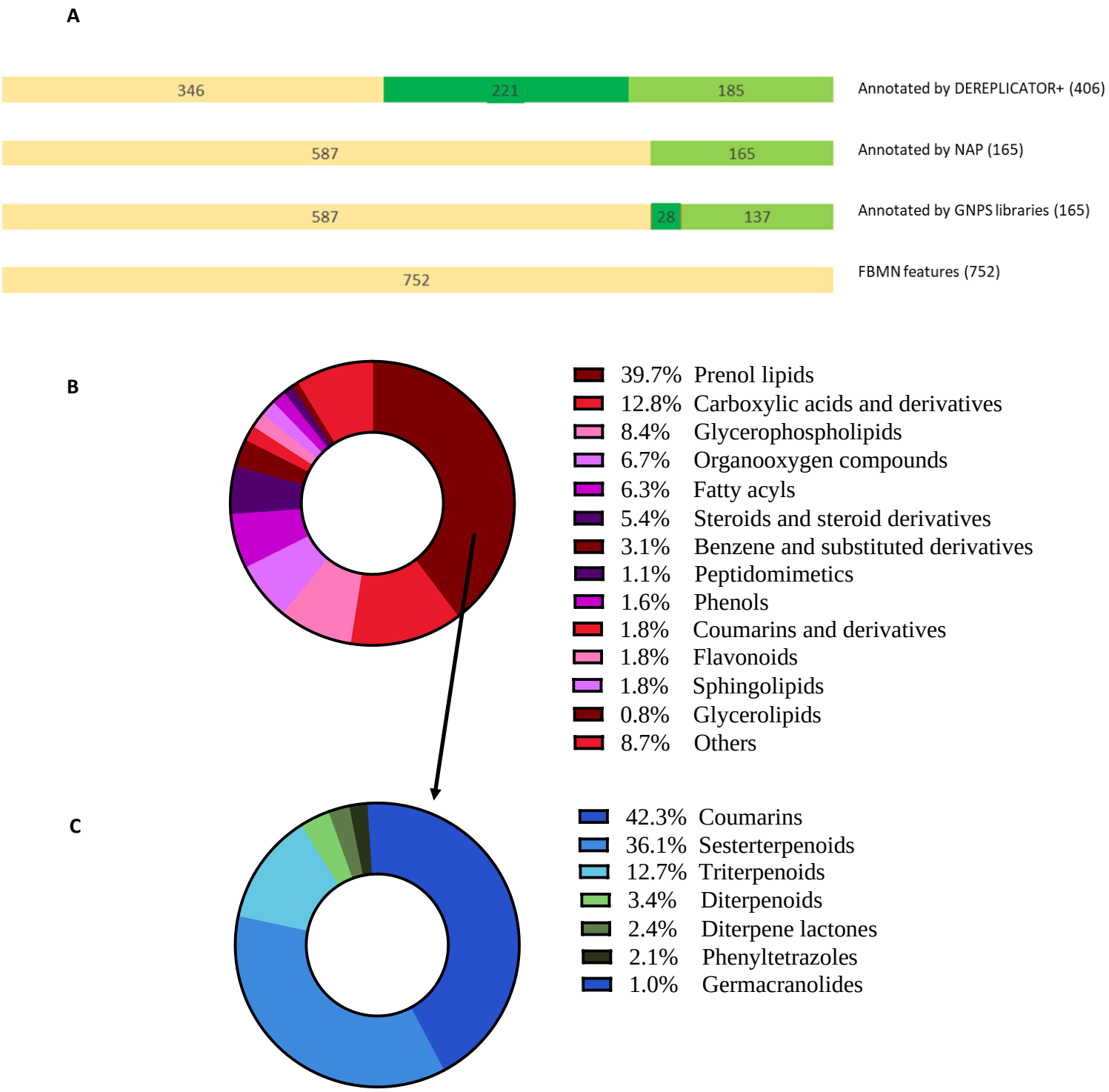

Fig. 3. (A) Annotation results obtained from *Hericium* FBMN analysis using GNPS libraries, DEREPLICATOR+ and NAP. The yellow color represents number of detected features, Green color the annotated features and dark green color the annotated features with score higher than 0.95 for GNPS libraries and higher than 12 for DEREPLECATOR plus database (B) Chemical classification (using ClassyFire) of the molecular families obtained from the *Hericium* FBMN. (C) Molecular distribution of the prenol lipids obtained from *Hericium* FBMN.

Several ergostane derivatives had been previously isolated from *H. erinaceus*, and some of their biological activities reported, such as anti-inflammatory effects and activation of the transcriptional activity of peroxisome proliferator-activated receptors (PPARs)[41]. Compounds that modulate the functions of PPARs are beneficial for the treatment of type 2 diabetes, obesity, metabolic syndromes, inflammation, and cardiovascular disease [42]. In our study, one molecular family contained derivatives and analogs of interesting secondary metabolites belonging to the ergostane-type sterol fatty acid esters as annotated by both DEREPLICATOR+ and SNAP-MS. The nodes of the molecular family showed that these compounds are not specific to *H. erinaceus* but were detected in both *Hericium* and *Pleurotus* in both the FB and mycelium (Fig. 4). In contrast to the ergostane family, most of the other secondary metabolites were unique to *Hericium* FB or *Hericium* mycelium.

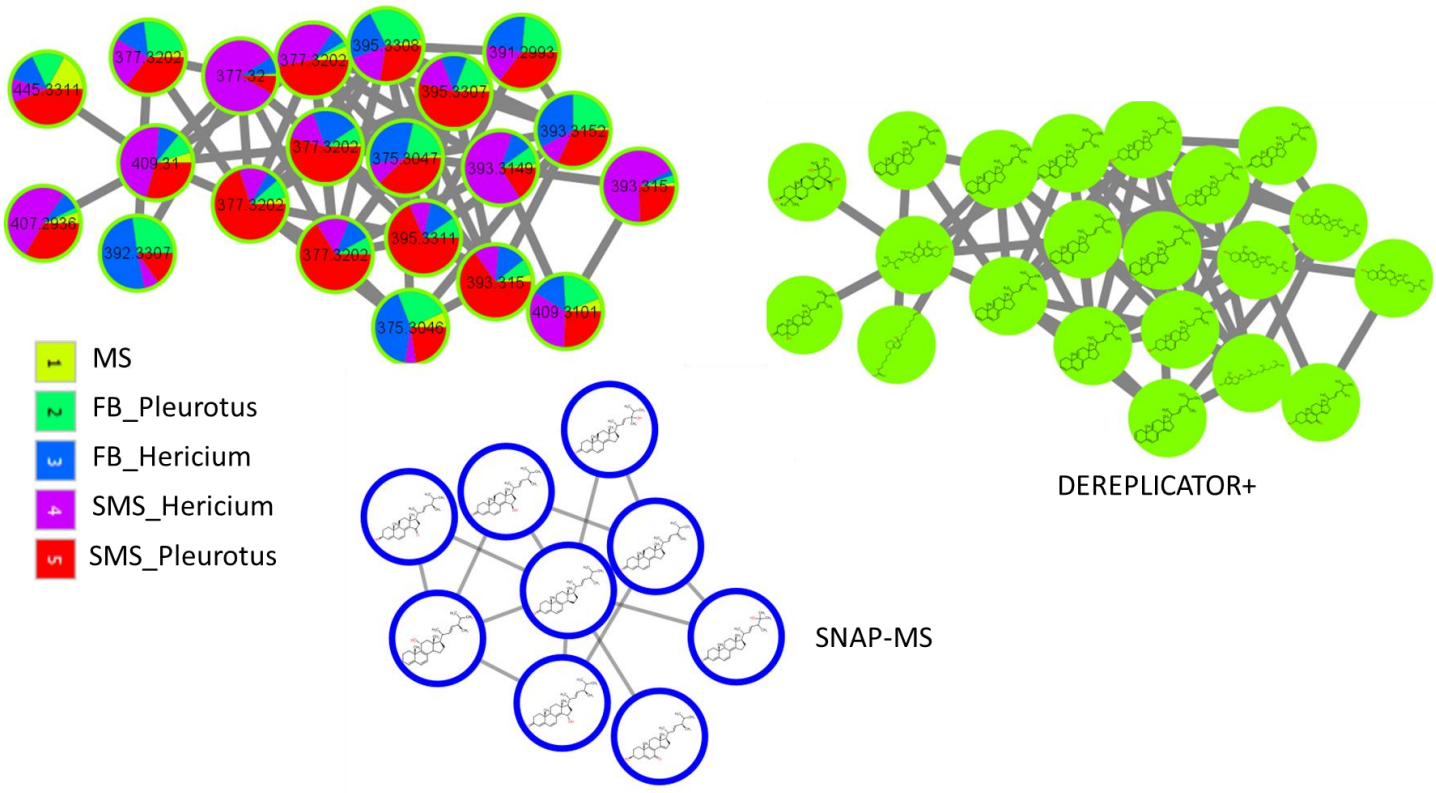

Fig. 4. Molecular families from the FBMN results, with most components detected in both *Hericium* and *Pleurotus* fruiting bodies (FB) and mycelium (SMS). Most of the components were annotated as ergosterol derivatives and analogs using both DEREPLICATOR+ and SNAP-MS such as, Ergosta-5,7,9(11),22-tetraen-3β-ol, Ergosta-3,5,7,9(11),22-pentaene and Citreoanthrasteroid_B.

It has been reported that more than 80 bioactive secondary metabolites are unique to *H. erinaceus* FB or mycelium with antitumor, antibacterial, hypoglycemic and neuroprotective effects[25,43,44]. These specialized secondary metabolites include structure families of erinacerins, erinacines, hericenones, hirecenes and ergostanes. In our study, none of these reported metabolites were annotated using GNPS libraries or NAP; however, using DEREPLICATOR+ and SNAP-MS methods, 14 and 26 of the metabolites mentioned above were annotated, respectively (Fig. 5).

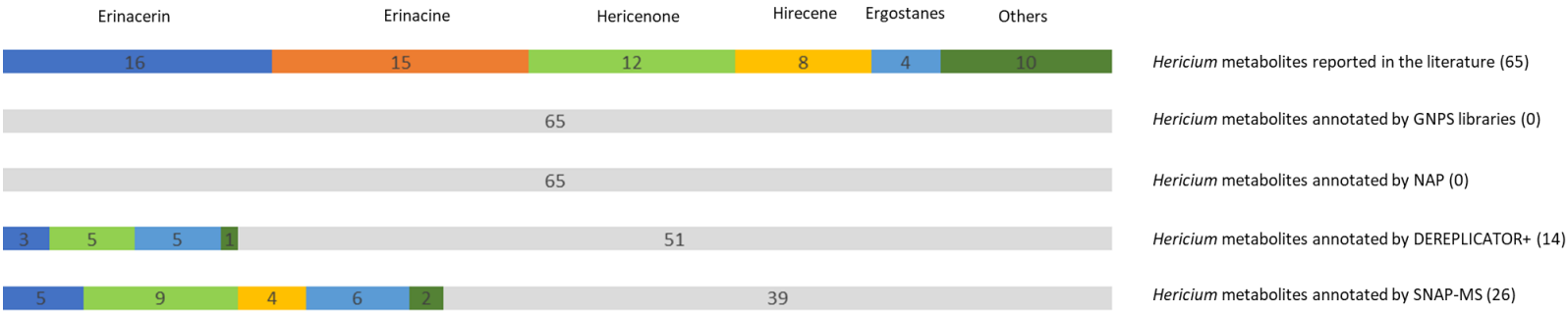

Fig. 5. Unique metabolite families isolated from *Hericium erinaceus* and annotated using GNPS libraries, NAP, DEREPLICATOR+ and SNAP-MS.

Hericenones are unique specialized metabolites; more than 10 hericenone compounds (A–J) and isohericenone J were isolated from the FB of *H. erinaceus*. Hericenones C, D and E have been reported to have a stimulatory effect on the synthesis of nerve growth factor[45], hericenone F to have anti-inflammatory activity[46], and hericenone J and isohericenone J to have anticancer activities[47].

In accordance with the literature, our FBMN results showed two molecular families that were unique to the *Hericium* FB extracts[48]. Their components were classified to belong to hericenone derivatives and analogs as annotated by DEREPLICATOR+ and SNAP-MS. Five hericenones were annotated using DEREPLICATOR+ and nine using SNAP-MS. MS2LDA results showed that the nodes of the molecular family in Fig. 6A share the unsupervised Mass2Motifs 231 and 155 (tentative substructure annotations in Fig. S6). The molecular family in Fig. 6B contains hericenone J analogs (m/z = 317.1745), as annotated by SNAP-MS. In accordance with the FERMO results, most of the nodes of these two molecular families were upregulated by increasing the OMSW percentage in the mushroom substrate.

Erinacerins are also unique secondary metabolites for their ability to inhibit α-glucosidase[49]. More than 15 erinacerins (A-O) were isolated from the *H. erinaceus* mycelium. In accordance with the

literature, our FBMN results showed that most of the annotated erinacerins and their analogs, using DEREPLICATOR+ and SNAP-MS, were isolated from the SMS which contains the mycelium[50,51]. In addition, some of the molecular family nodes related to erinacerin analogs were upregulated by increasing the OMSW percentage in the mushroom substrate (Fig. 6C).

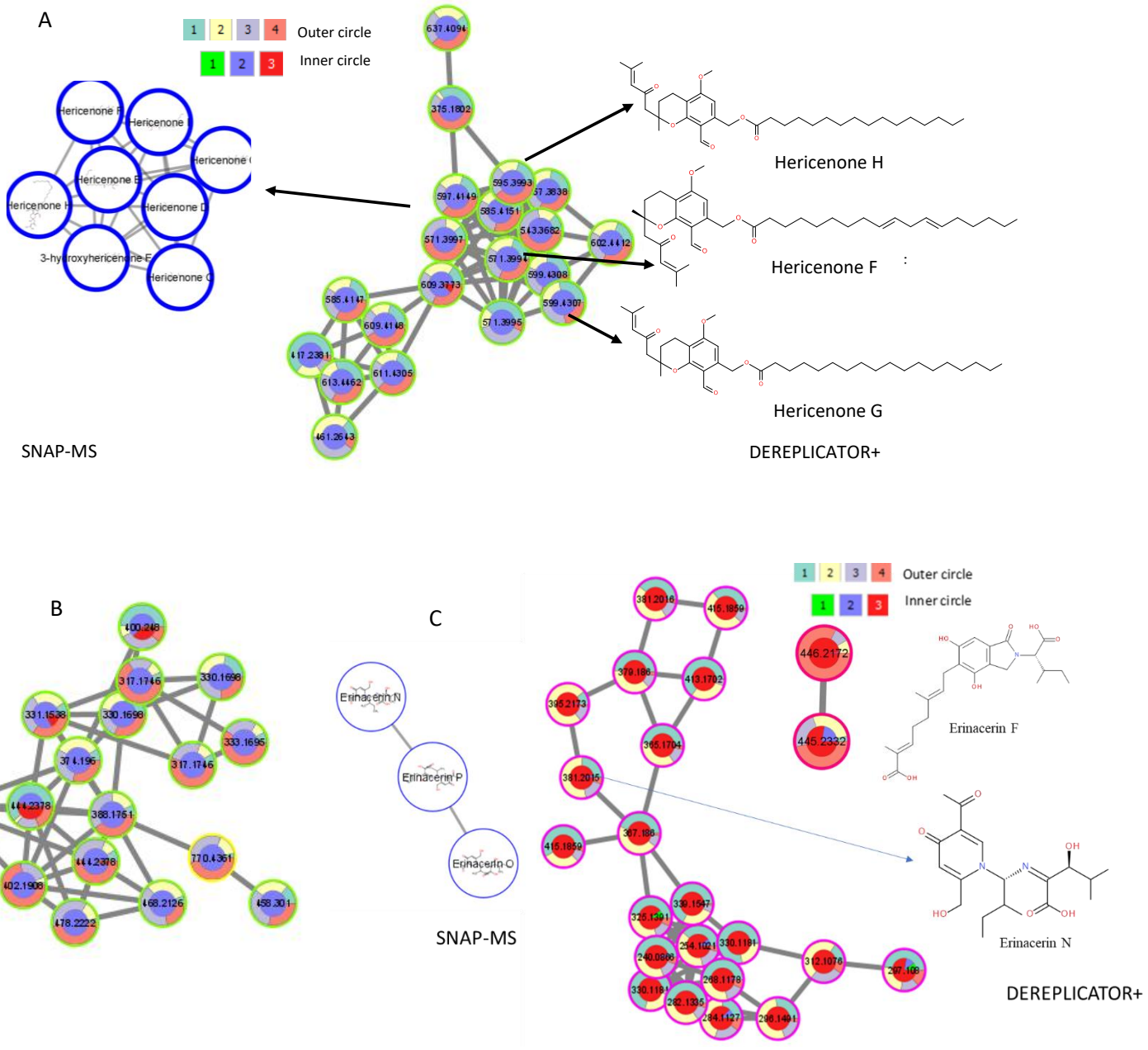

Fig. 6. Cytoscape visualization of the molecular features analyzed by FBMN mass spectral similarity networking. Colors of the inner circle represent features detected in the mushroom substrate (MS), fruiting body (FB) and spent

mushroom substrate (SMS) – 1, 2 and 3, respectively. Colors of the outer circle represent features detected in the groups of 0, 33, 60 and 80% OMSW – 1, 2, 3 and 4, respectively. (A and B) Molecular families whose components were detected mostly in the FB and increased with increasing OMSW percentage. (C) Molecular families whose components were detected mostly in the mycelium, some of them increasing with the addition of OMSW.

Another two molecular families detected in the *Hericium* FB extracts and the nodes of one of the molecular families were classified as belonging to enniatin derivatives and analogs as annotated by SNAP-MS (Fig. 7A). Enniatins are toxic due to their ability to act as ionophores, changing ion transport across membranes and disrupting the ionic selectivity of cell walls. In the membrane, enniatins form a dimeric structure which transports ions (especially K^+, Mg^{2+}, Ca^{2+} and Na^+) across membranes. The other molecular family components were not annotated (Fig. 7B). In accordance with the FERMO results, the compounds related to these two molecular families were downregulated by the addition of OMSW, and most of their metabolites only appeared in the 0% OMSW group (Fig. 7).

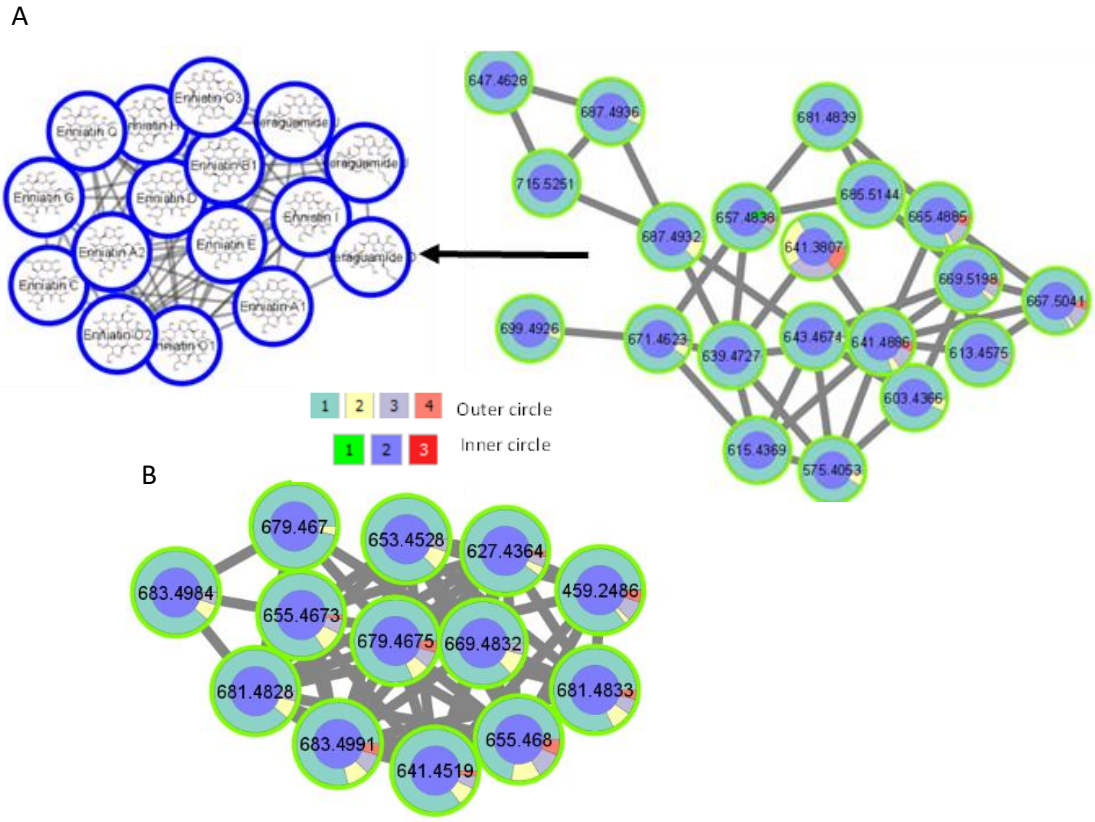

Fig. 7. Molecular families from FBMN analysis whose components appeared mainly in the 0% OMSW group. Colors of the inner circle represent features detected in the mushroom substrate (MS), fruiting body (FB) and spent mushroom substrate (SMS) – 1, 2 and 3, respectively. Colors of the outer circle represent features detected in the groups of 0, 33, 60 and 80% OMSW – 1, 2, 3 and 4, respectively. (A) Molecular family annotated by SNAP-MS as enniatins. (B) Molecular family whose components were not annotated by SNAP-MS.

Final discussion and conclusions

Computational metabolomics strategies were used for LC-MS/MS data processing and handling to analyze the effect of mixing mushroom substrates with OMSW on *Hericium* and *Pleurotus* specialized metabolic diversity. *Hericium* FB and mycelium were more enriched with specialized secondary metabolites than *Pleurotus* FB and mycelium. FERMO and FBMN results showed that OMSW increased the content of specialized secondary metabolites belonging to the hericenone and erinacerin families in *Hericium* FB and mycelium, respectively. These specialized metabolites have been reported to support health due to their anti-inflammatory, anticancer and neuroprotective properties. The addition of OMSW was further found to decrease the levels of toxic metabolites related to the enniatin family. Altogether, we demonstrate how untargeted metabolomics measurements in combination with computational metabolomics strategies offer a versatile approach to prioritize and structurally annotate affected specialized metabolite families. Given the complexity of most specialized microbial and plant metabolomes, up-to-date mass spectral libraries together with state-of-the-art computational metabolomics strategies are unlikely to cover all metabolites in the natural extracts; however, our analysis demonstrates an innovative approach for the better understanding their chemical complexities. We do note that the use of various complementary tools can be cumbersome due to their various input demands and parameter settings; however, their complementary perspectives do provide additive value. Furthermore, platforms like FERMO and MolNetEnhancer together with Cytoscape start to bring together analyses and annotation results. Altogether, the computational metabolomics strategies allowed for an in-depth study of the mushroom specialized metabolome and the impact of substrate additives thereon. Additionally, our study was confirmed the positive effect of OMSW on mushroom growth as earlier observed in literature. In conclusion, our study highlights the need for careful consideration of the impact of new nutritional resources, be it beneficial, neutral, or harmful, on the metabolic content of mushrooms or other biological products.

Acknowledgements

The authors thank Niek F. de Jonge - Bioinformatics Group, Wageningen University & Research, NL, for MS2Query development and integrating it into the FERMO dashboard. The authors also express their gratitude to the developers of the community-based open-source metabolomics tools that were used in our study.

Authors Contributions

I.P. and N.E. grow the mushrooms; E.K. extracted the metabolites; R.S. performed the LC-MS/MS measurements; S.K. performed the data and computational metabolomics analysis; M.Z. developed FERMO platform; JJJvdH supervised the research; S.K. wrote the first draft of the manuscript; S.K., I.P. and JJJvdH writing—review and editing. All authors have read and agreed to the final version of the manuscript.

Competing Interests

JJJvdH is a member of the Scientific Advisory Board of NAICONS Srl., Milano, Italy, and is consulting for Corteva Agriscience, Indianapolis, IN, USA. All other authors declare to have no competing interests.

References

1. Mapook A, Hyde KD, Hassan K, et al. Ten decadal advances in fungal biology leading towards human well-being. Fungal Divers 2022;116:547-614.
2. Rai SN, Mishra D, Singh P, Vamanu E, Singh MP. Therapeutic applications of mushrooms and their biomolecules along with a glimpse of in silico approach in neurodegenerative diseases. Biomedicine & Pharmacotherapy 2021;137:111377.
3. Phan CW, David P, Naidu M, Wong KH, Sabaratnam V. Therapeutic potential of culinary-medicinal mushrooms for the management of neurodegenerative diseases: diversity, metabolite, and mechanism. Crit Rev Biotechnol 2015;35:355-68.
4. Meena MG, Lane MJ, Tannous J, et al. A guidance into the fungal metabolomic abyss: Network analysis for revealing relationships between exogenous compounds and their outputs. bioRxiv 2022:2022.08.11.503656.
5. Chen P, Yong Y, Gu Y, Wang Z, Zhang S, Lu L. Comparison of antioxidant and antiproliferation activities of polysaccharides from eight species of medicinal mushrooms. Int J Med Mushrooms 2015;17:287-95.
6. Thongbai B, Rapior S, Hyde KD, Wittstein K, Stadler M. Hericium erinaceus, an amazing medicinal mushroom. Mycological Progress 2015;14:91.
7. Friedman M. Chemistry, Nutrition, and Health-Promoting Properties of Hericium erinaceus (Lion's Mane) Mushroom Fruiting Bodies and Mycelia and Their Bioactive Compounds. Journal of Agricultural and Food Chemistry 2015;63:7108-23.
8. Chong PS, Fung ML, Wong KH, Lim LW. Therapeutic Potential of Hericium erinaceus for Depressive Disorder. Int J Mol Sci 2019;21.
9. Nagano M, Shimizu K, Kondo R, et al. Reduction of depression and anxiety by 4 weeks <I>Hericium erinaceus</I> intake. Biomedical Research 2010;31:231-7.
10. Yi Z, Shao-long Y, Ai-hong W, et al. Protective Effect of Ethanol Extracts of Hericium erinaceus on Alloxan-Induced Diabetic Neuropathic Pain in Rats. Evidence-Based Complementary and Alternative Medicine 2015;2015:595480.
11. Rahman MA, Abdullah N, Aminudin N. Inhibitory Effect on In Vitro LDL Oxidation and HMG Co-A Reductase Activity of the Liquid-Liquid Partitioned Fractions of Hericium erinaceus (Bull.) Persoon (Lion's Mane Mushroom). BioMed Research International 2014;2014:828149.

12. Tsai-Teng T, Chin-Chu C, Li-Ya L, et al. Erinacine A-enriched Hericium erinaceus mycelium ameliorates Alzheimer's disease-related pathologies in APPswe/PS1dE9 transgenic mice. Journal of Biomedical Science 2016;23:49.
13. Mizuno T, Wasa T, Ito H, Suzuki C, Ukai N. Antitumor-active Polysaccharides Isolated from the Fruiting Body of Hericium erinaceum, an Edible and Medicinal Mushroom Called yamabushitake or houtou. Bioscience, Biotechnology, and Biochemistry 1992;56:347-8.
14. Ma B-J, Shen J-W, Yu H-Y, Ruan Y, Wu T-T, Zhao X. Hericenones and erinacines: stimulators of nerve growth factor (NGF) biosynthesis in Hericium erinaceus. Mycology 2010;1:92-8.
15. Zhiming F, Yi L, Qiang Z. A Potent Pharmacological Mushroom: *Pleurotus eryngii*. Fungal Genomics & Biology 2016;6:1-5.
16. Wang S-j, Li Y-x, Bao L, et al. Eryngiolide A, a Cytotoxic Macrocyclic Diterpenoid with an Unusual Cyclododecane Core Skeleton Produced by the Edible Mushroom Pleurotus eryngii. Organic Letters 2012;14:3672-5.
17. Jing X, Mao D, Geng L, Xu C. Medium optimization, molecular characterization, and bioactivity of exopolysaccharides from Pleurotus eryngii. Arch Microbiol 2013;195:749-57.
18. Zervakis GI, Koutrotsios G, Katsaris P. Composted versus raw olive mill waste as substrates for the production of medicinal mushrooms: an assessment of selected cultivation and quality parameters. Biomed Res Int 2013;2013:546830.
19. Ruiz-Rodriguez A, Soler-Rivas C, Polonia I, Wichers HJ. Effect of olive mill waste (OMW) supplementation to Oyster mushrooms substrates on the cultivation parameters and fruiting bodies quality. International Biodeterioration & Biodegradation 2010;64:638-45.
20. Christoforou E, Fokaides PA. A review of olive mill solid wastes to energy utilization techniques. Waste Management 2016;49:346-63.
21. Ouazzane H, Laajine F, El Yamani M, et al. Olive Mill Solid Waste Characterization and Recycling opportunities : A review. Journal of Materials and Environmental Sciences 2017;8:2632-50.
22. Mkhize SS, Cedric Simelane MB, Mongalo IN, Pooe OJ. The Effect of Supplementing Mushroom Growing Substrates on the Bioactive Compounds, Antimicrobial Activity, and Antioxidant Activity of Pleurotus ostreatus. Biochemistry Research International 2022;2022:9436614.
23. Kinge TR, Adi EM, Mih AM, Ache NA, Nji TM. Effect of substrate on the growth, nutritional and bioactive components of Pleurotus ostreatus and Pleurotus florida. African Journal of Biotechnology 2016;15:1476-86.
24. Avni S, Ezove N, Hanani H, et al. Olive Mill Waste Enhances α-Glucan Content in the Edible Mushroom Pleurotus eryngii. Int J Mol Sci 2017;18.
25. Yang F, Wang H, Feng G, Zhang S, Wang J, Cui L. Rapid Identification of Chemical Constituents in Hericium erinaceus Based on LC-MS/MS Metabolomics. Journal of Food Quality 2021;2021:5560626.
26. Satria D, Tamrakar S, Suhara H, Kaneko S, Shimizu K. Mass Spectrometry-Based Untargeted Metabolomics and α-Glucosidase Inhibitory Activity of Lingzhi (Ganoderma lingzhi) During the Developmental Stages. Molecules 2019;24:2044.
27. Ebbels TMD, van der Hooft JJJ, Chatelaine H, et al. Recent advances in mass spectrometry-based computational metabolomics. Current Opinion in Chemical Biology 2023;74:102288.
28. Uppal K, Walker DI, Liu K, Li S, Go YM, Jones DP. Computational Metabolomics: A Framework for the Million Metabolome. Chem Res Toxicol 2016;29:1956-75.
29. Wang M, Carver JJ, Phelan VV, et al. Sharing and community curation of mass spectrometry data with Global Natural Products Social Molecular Networking. Nature Biotechnology 2016;34:828-37.
30. Schmid R, Heuckeroth S, Korf A, et al. Integrative analysis of multimodal mass spectrometry data in MZmine 3. Nature Biotechnology 2023;41:447-9.
31. Mitja MZ, Lina MBM, Hannah EA, et al. FERMO: a Dashboard for Streamlined Rationalized Prioritization of Molecular Features from Mass Spectrometry Data. bioRxiv 2022:2022.12.21.521422.
32. de Jonge NF, Louwen JJR, Chekmeneva E, et al. MS2Query: reliable and scalable MS2 mass spectra-based analogue search. Nature Communications 2023;14:1752.

33. Louis Felix N, Daniel P, Robin S, et al. Feature-based Molecular Networking in the GNPS Analysis Environment. bioRxiv 2019:812404.
34. Horai H, Arita M, Kanaya S, et al. MassBank: a public repository for sharing mass spectral data for life sciences. J Mass Spectrom 2010;45:703-14.
35. Mohimani H, Gurevich A, Shlemov A, et al. Dereplication of microbial metabolites through database search of mass spectra. Nature Communications 2018;9:4035.
36. da Silva RR, Wang M, Nothias LF, et al. Propagating annotations of molecular networks using in silico fragmentation. PLoS Comput Biol 2018;14:e1006089.
37. Morehouse NJ, Clark TN, McMann EJ, et al. Annotation of natural product compound families using molecular networking topology and structural similarity fingerprinting. Nature Communications 2023;14:308.
38. Shannon P, Markiel A, Ozier O, et al. Cytoscape: a software environment for integrated models of biomolecular interaction networks. Genome Res 2003;13:2498-504.
39. Ernst M, Kang KB, Caraballo-Rodríguez AM, et al. MolNetEnhancer: Enhanced Molecular Networks by Integrating Metabolome Mining and Annotation Tools. Metabolites 2019;9:144.
40. Djoumbou Feunang Y, Eisner R, Knox C, et al. ClassyFire: automated chemical classification with a comprehensive, computable taxonomy. Journal of Cheminformatics 2016;8:61.
41. Li W, Zhou W, Song SB, Shim SH, Kim YH. Sterol Fatty Acid Esters from the Mushroom Hericium erinaceum and Their PPAR Transactivational Effects. Journal of Natural Products 2014;77:2611-8.
42. Kuroda M, Mimaki Y, Honda S, Tanaka H, Yokota S, Mae T. Phenolics from Glycyrrhiza glabra roots and their PPAR-gamma ligand-binding activity. Bioorg Med Chem 2010;18:962-70.
43. Chen J, Zeng X, Yang YL, et al. Genomic and transcriptomic analyses reveal differential regulation of diverse terpenoid and polyketides secondary metabolites in Hericium erinaceus. Scientific Reports 2017;7:10151.
44. Corana F, Cesaroni V, Mannucci B, et al. Array of Metabolites in Italian Hericium erinaceus Mycelium, Primordium, and Sporophore. Molecules 2019;24.
45. Brandalise F, Roda E, Ratto D, et al. Hericium erinaceus in Neurodegenerative Diseases: From Bench to Bedside and Beyond, How Far from the Shoreline? J Fungi (Basel) 2023;9.
46. Xie G, Tang L, Xie Y, Xie L. Secondary Metabolites from Hericium erinaceus and Their Anti-Inflammatory Activities. Molecules 2022;27.
47. Li W, Zhou W, Kim EJ, Shim SH, Kang HK, Kim YH. Isolation and identification of aromatic compounds in Lion's Mane Mushroom and their anticancer activities. Food Chem 2015;170:336-42.
48. Ma B-J, Yu H-Y, Shen J-W, et al. Cytotoxic aromatic compounds from Hericium erinaceum. The Journal of Antibiotics 2010;63:713-5.
49. Wang K, Bao L, Qi Q, et al. Erinacerins C-L, isoindolin-1-ones with α-glucosidase inhibitory activity from cultures of the medicinal mushroom Hericium erinaceus. J Nat Prod 2015;78:146-54.
50. Lee EW, Shizuki K, Hosokawa S, et al. Two novel diterpenoids, erinacines H and I from the mycelia of Hericium erinaceum. Biosci Biotechnol Biochem 2000;64:2402-5.
51. Kawagishi H, Masui A, Tokuyama S, Nakamura T. Erinacines J and K from the mycelia of Hericium erinaceum. Tetrahedron 2006;62:8463-6.